Computing Call-Blocking Probabilities in LEO Satellite Constellations

Abdul Halim Zaim, Harry G. Perros, *Senior Member, IEEE*, and George N. Rouskas, *Senior Member, IEEE*

***Abstract*—We present an analytical model for computing call-blocking probabilities in a low earth orbit (LEO) satellite network that carries voice calls. Both satellite- and earth-fixed constellations with interorbit links and handoffs are considered. In this model, we assume a single beam per satellite. Also, we assume that call arrivals are Poisson with a fixed arrival rate that is independent of the geographic area. The model is analyzed approximately by decomposing it into subsystems. Each subsystem is solved in isolation exactly using a Markov process and the individual results are combined together through an iterative method. Numerical results demonstrate that our method is accurate for a wide range of traffic patterns. We also derive an upper and lower bound for the link-blocking probabilities that can be computed efficiently. These bounds can be used for constellations of realistic size where each satellite has multiple beams.**

***Index Terms*—Call blocking; handoffs; low earth orbit (LEO) satellite constellations.**

I. Introduction

RECENT advances in satellite communications make it possible to use satellites as an alternative to wireless telephones and networks. The 20th century witnessed the development of satellite communication systems aimed at providing mobile telephony and data-transmission services. These services are globally available and are independent from terrestrial networks. Satellite systems are location insensitive and can be used to extend the reach of networks and applications to anywhere on the earth with a fixed constellation cost.

A low earth orbit (LEO) or medium earth orbit (MEO) satellite system is a set of identical satellites that are launched in several orbital planes, with the orbits having the same altitude. The satellites move in a synchronized manner in trajectories relative to the earth. Such a set of satellites is referred to as a *constellation*. The position of all the satellites in relation to the earth at some instance of time repeats itself after a predetermined period, called a*system period*, which is usually several days. A satellite within an orbit also comes to the same point on the sky relative to the earth after a certain time, called the *orbit period*, which is approximately 100 minutes for LEO systems. If satellites are equipped with advanced onboard processing, they can communicate directly with each other by line of sight using intersatellite links (ISL). If the ISL is between satellites on the same orbit, it is called intraplane ISL and if it is between satellites in adjacent planes it is called interplane ISL. The use of ISLs gives the chance of routing in the sky and, therefore, increases the flexibility of the system. Although ISLs require complex call-management functions due to the dynamic nature of the constellation, they move the burden of the network from ground to space since they permit two users in different footprints to communicate without the need for a terrestrial system.

Depending on the antenna technology used, satellite constellations can provide one of two types of coverage. If the satellite antenna is fixed as the satellite moves along its orbit, then the coverage is called *satellite fixed*. In this case, the footprint area moves along with the satellite. In *earth-fixed coverage*, the earth's surface is divided into cells as in a terrestrial cellular system and a cell is serviced continuously by the same beam during the entire time that the cell is within the footprint area of the satellite. This type of coverage requires an antenna that tracks the cell area.

In a LEO/MEO satellite network, the frequency of handoffs depends on the beam size, call duration, footprint size, and satellite speed. A handoff may be from one beam to another (beam handoff) or from one satellite to another (satellite handoff). In an earth-fixed system, both satellite and beam handoffs occur at periodic intervals, when a beam or satellite is assigned to a new cell. During the handoff, all beams are reassigned to their respective cells in the adjacent footprint area. However, in a satellite-fixed system, a handoff may occur at any point in time. Since a call handed over to another beam may be dropped if there is not enough bandwidth on that beam to carry the call, handoffs in satellite-fixed systems must be carefully handled to prevent a degradation in the quality of service. Finally, we note that LEO satellites rotate around the earth much faster than any object on the surface of the earth. Therefore, the movement of objects can be considered negligible and we assume that handoffs occur due only to the movement of satellites.

Existing and planned LEO/MEO satellite systems for worldwide mobile telephony include Globalstar, Iridium, ICO, Ellipso, Constellation, Courier, and Gonets. (A survey of LEO systems can be found in [3].) These systems differ in many aspects, including the number of orbits and of satellites per orbit, the number of beams per satellite, their capacity, the band they operate (S-Band, L-Band, etc.), and the access method employed (FDMA, TDMA, or CDMA). Also, these systems provide different services and may or may not have onboard switching capabilities. For instance, Iridium has onboard digital processing and switching, while other systems, such as the Globalstar, act as a bent pipe. Despite these differences, from the point of view of providing telephony-based services,

Manuscript received September 11, 2001; revised January 31, 2002.

The authors are with the Department of Computer Science, North Carolina State University, Raleigh, NC 27695-7534 USA (e-mail: ahzaim@csc.ncsu.edu; hp@csc.ncsu.edu; rouskas@csc.ncsu.edu).

Digital Object Identifier 10.1109/TVT.2003.811219

the principles of operation are very similar and, thus, the analytical techniques to be developed in the proposed work are applicable to any LEO/MEO satellite system that offers such services.

The performance of satellite systems has been studied by several authors. In general, most studies rely on simple queueing models to evaluate call-blocking probabilities and focus on devising methods for improving the performance of calls during handoffs (e.g., by assigning higher priority to handoff calls, using guard channels, or making reservations ahead of a handoff instant). In [2], Ganz *et al.* expressed the system performance in terms of the *distribution of the number of handoffs* occurring during a single transaction time and the *average call-drop probability*. In their work, each cell is modeled as an *M/M/K/K* queue where *K* denotes the number of channels per cell, assuming that the number of handoff calls entering a cell is equal to the number of handoff calls leaving the cell. Del Re *et al.* in [7] and [6], proposed an analytical model to analyze handoff queueing strategies under fixed channel allocation. Their method is designed for satellite-fixed cell coverage. In [5], Pennoni and Ferroni described an algorithm to improve the performance of handoffs in LEO systems. They defined two queues for each cell, one for new calls and one for handoff calls. The calls are held in these two queues for a maximum allowed waiting time. The handoff queue has higher priority than the new-calls queue. In [1], Dosiere *et al.* used the same model to calculate the handoff traffic rate over a street of coverage. Once the handoff arrival rate has been calculated as in [5], the total arrival rate is computed as the summation of the new-call and handoff arrival rates. In [9], Ruiz *et al.* used a technique similar to the one used in [5]. However, this time they used some guard channels for handoff calls and they distinguished between the new-arrival rate and handoff-attempt rates. In [8], Respero and Maral defined a guaranteed handoff mechanism for LEO satellite systems with satellite-fixed cell configuration. In this method, channel reservation is performed according to the location of the user. The advantage of this method is that the reservation is done only on the next satellite, rather than on the whole call path. With this approach, the amount of redundant circuitry is minimized and the handoff success rate is as high as the static reservation technique. In [10], Wan *et al.* defined a channel-reservation algorithm for handoff calls. In this algorithm, they keep three queues: one for handoff requests, one for new call requests, and one for available channels. Each request comes with the information indicating the position of the user within the footprint area. The position information is then used to calculate the time of the next handoff. The aim of the algorithm is to match the available channels with the handoff and new-call request queues according to the time criteria. A similar approach is proposed by Obradovic and Cigoj in [4]. They proposed a dynamic channel-reservation scheme. Handoff management is performed with two queues: one for handoff requests and one for new call requests. Available channels are also divided into two subgroups: reserved and nonreserved ones. Reserved channels have priority over nonreserved channels during the assignment.

In [11], the authors proposed an approximation method for calculating call-blocking probabilities in a group of LEO/MEO satellites arranged in a single orbit. Both satellite- and earth-fixed types of coverage with handoffs were considered. In the model, it was assumed that each satellite has a single beam and that the arrival process is Poisson with a rate independent of the geographic area. The model was analyzed using decomposition. Specifically, the entire orbit is decomposed into subsystems, each consisting of a small number of satellites. Each subsystem is analyzed exactly, by observing that its steady-state probability distribution has a product-form solution. An efficient algorithm was proposed to calculate the normalizing constant associated with this product-form solution. The results obtained from each subsystem are combined together in an iterative manner in order to solve the entire orbit.

In this paper, we generalize the above algorithm to an entire constellation of LEO/MEO satellites involving multiple orbits. We consider both satellite- and earth-fixed constellations with interorbit links and handoffs. We assume that each satellite employs a single beam and that calls arrive in a Poisson fashion with a fixed arrival rate independent of the geographical area. We present an approximate decomposition algorithm for the calculation of the call-blocking probabilities in a LEO/MEO satellite constellation. Specifically, the entire constellation is decomposed into subsystems and each subsystem is analyzed exactly as a Markov process by using the solution technique presented in [11]. This approach leads to an iterative scheme where the individual subsystems are solved successively until a convergence criterion is satisfied. We also derive upper and lower bounds on the link-blocking probabilities. These bounds are computed efficiently and can be useful for large satellite constellations when each satellite employs multiple beams.

The paper is organized as follows. In Section II, we present briefly an exact Markov process model under the assumption that satellites are fixed in the sky (i.e., no handoffs take place) and in Section III we present an approximate decomposition algorithm for a constellation of satellites. In Section IV, we extend our approach to model handoffs for both earth- and satellite-fixed coverage and in Section V we derive efficient upper and lower bounds on the call-blocking probabilities. We present numerical results in Section VI and in Section VII we conclude the paper.

II. An Exact Model for the No-Handoffs Case

In this section, we briefly review the single-orbit model proposed in [11]. This model is used in the decomposition algorithm described in the following section.

Let us consider a single orbit of a constellation and let us assume that the position of the satellites is fixed in the sky, as in the case of geostationary satellites. The analysis of such a system is simpler since no calls are lost due to handoffs from one satellite to another, as when the satellites move with respect to the users on the earth. This model is used in Section IV to model both earth- and satellite-fixed systems with handoffs.

Each up-and-down link (UDL) of a satellite has the capacity to support up to C_{UDL} bidirectional calls, while each ISL has the capacity equal to C_{ISL} bidirectional calls. We assume that call requests arrive at each satellite according to a Poisson process and that call-holding times are exponentially distributed. We now show how to compute blocking probabilities for the three

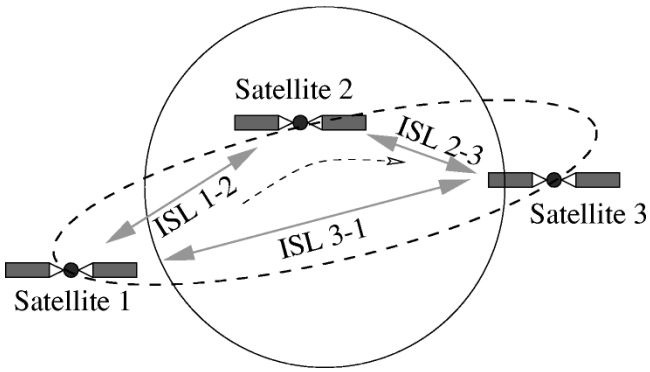

Fig. 1. Three satellites in a single orbit.

satellites in the single orbit of Fig. 1. The analysis can be generalized to analyze $k > 3$ satellites in a single orbit. For simplicity, we consider only shortest-path routing, although the analysis can be applied to any fixed routing scheme whereby the path taken by a call is fixed and known in advance of the arrival of the call request.

Let n_{ij} be a random variable representing the number of active bidirectional calls between satellite i and satellite j, $1 \leq i, j \leq 3$ regardless of whether the calls originated at satellite i or j. As an example, if $n_{12} = 1$, then there is one call using a one-way ISL channel from satellite 1 to satellite 2 and a one-way ISL channel from satellite 2 to satellite 1. If $n_{11} = 1$, then there is a call between a customer under satellite 1 and a customer also under satellite 1 and two bidirectional UDL channels are used. Let λ_{ij} (respectively, $1/\mu_{ij}$) denote the arrival rate (respectively, mean holding time) of calls between satellites i and j. Then, the three-satellite system in Fig. 1 can be described by the six-dimensional Markov process as

$$\underline{n} = (n_{11}, n_{12}, n_{13}, n_{22}, n_{23}, n_{33}). \tag{1}$$

Also, let $\underline{1}_{ij}$ denote a vector with zeros for all random variables except random variable n_{ij}, which is 1. The state transition rates for this Markov process are given by

$$r(\underline{n}, \underline{n} + \underline{1}_{ij}) = \lambda_{ij} \qquad \forall i, j \tag{2}$$

$$r(\underline{n}, \underline{n} - \underline{1}_{ij}) = n_{ij}\mu_{ij} \qquad \forall i, j, n_{ij} > 0. \tag{3}$$

The transition in (2) is due to the arrival of a call between satellites i and j, while the transition in (3) is due to the termination of a call between satellites i and j.

Let Ω denote the state space for this Markov process. Due to the fact that some of the calls share common UDL and intersatellite links, the following constraints are imposed on Ω:

$$2n_{11} + n_{12} + n_{13} \leq C_{\text{UDL}} \tag{4}$$

$$n_{12} + 2n_{22} + n_{23} \leq C_{\text{UDL}} \tag{5}$$

$$n_{13} + n_{23} + 2n_{33} \leq C_{\text{UDL}} \tag{6}$$

$$n_{12} \leq C_{\text{ISL}} \tag{7}$$

$$n_{13} \leq C_{\text{ISL}} \tag{8}$$

$$n_{23} \leq C_{\text{ISL}}. \tag{9}$$

Constraint (4) ensures that the number of calls originating (equivalently, terminating) at satellite 1 is at most equal to the capacity of the UDL of that satellite. Note that a call that originates and terminates within the footprint of satellite 1 captures two channels; thus, the term $2n_{11}$ in constraint (4). Constraints (5) and (6) are similar to (4), but correspond to satellites 2 and 3, respectively. Finally, constraints (7)–(9) ensure that the number of calls using the link between two satellites is at most equal to the capacity of that link. Note that, because of (4)–(6), constraints (7)–(9) become redundant when $C_{\text{ISL}} \geq C_{\text{UDL}}$. In other words, there is no blocking at the intersatellite links when the capacity of the links is at least equal to the capacity of the UDL at each satellite.[1]

It is straightforward to verify that the Markov process for the three-satellite system shown in Fig. 1 has a closed-form solution that is given by

$$P(\underline{n}) = P(n_{11}, n_{12}, n_{13}, n_{22}, n_{23}, n_{33}) = \frac{1}{G}\frac{\rho_{11}^{n_{11}}}{n_{11}!}\frac{\rho_{12}^{n_{12}}}{n_{12}!}\frac{\rho_{13}^{n_{13}}}{n_{13}!}\frac{\rho_{22}^{n_{22}}}{n_{22}!}\frac{\rho_{23}^{n_{23}}}{n_{23}!}\frac{\rho_{33}^{n_{33}}}{n_{33}!}, \quad \underline{n} \in \Omega \tag{10}$$

where G is the normalizing constant and $\rho_{ij} = \lambda_{ij}/\mu_{ij}$, $i, j = 1, 2, 3$ is the offered load of calls from satellite i to satellite j. As we can see, the solution is the product of six terms of the form $\rho_{ij}^{n_{ij}}/n_{ij}!$, $i, j = 1, 2, 3$, each corresponding to one of the six different source/destination pair of calls. Therefore, it is easily generalizable to a k-satellite system, $k > 3$.

An alternative way is to regard this Markov process as describing a network of six *M/M/K/K* queues, one for each source/destination pair of calls between the three satellites. Since the satellites do not move, there are no handoffs and as a consequence customers do not move from one queue to another (we will see in Section IV-B that handoffs may be modeled by allowing customers to move between the queues). Now, the probability that there are m customers in an *M/M/K/K* queue is given by the familiar expression $(\rho^m/m!)/\left(\sum_{l=0}^{K} \rho^l/l!\right)$ and, therefore, the probability that there are $(n_{11}, n_{12}, n_{13}, n_{22}, n_{23}, n_{33})$ customers in the six queues is given by (10). Unlike previous studies reported in the literature, our model takes into account the fact that the six *M/M/K/K* queues are not independent, since the number of customers accepted in each *M/M/K/K* queue depends on the number of customers in other queues, as described by the constraints (4)–(9).

Of course, the main concern in any product-form solution is the computation of the normalizing constant

$$G = \sum_{\underline{n} \in \Omega} \frac{\rho_{11}^{n_{11}}}{n_{11}!}\frac{\rho_{12}^{n_{12}}}{n_{12}!}\frac{\rho_{13}^{n_{13}}}{n_{13}!}\frac{\rho_{22}^{n_{22}}}{n_{22}!}\frac{\rho_{23}^{n_{23}}}{n_{23}!}\frac{\rho_{33}^{n_{33}}}{n_{33}!} \tag{11}$$

where the sum is taken over all vectors $\underline{n}$ that satisfy constraints (4) through (9). A procedure to compute the normalizing constant G in an efficient manner is presented in [11].

[1]When there are more than three satellites in an orbit, calls between a number of satellite pairs may share a given intersatellite link. Consequently, the constraints of a k-satellite orbit, $k > 3$, corresponding to (7)–(9), will be similar to constraints (4)–(6) in that the left-hand side will involve a summation over a number of calls. In this case, blocking on intersatellite links may occur even if $C_{\text{ISL}} \geq C_{\text{UDL}}$.

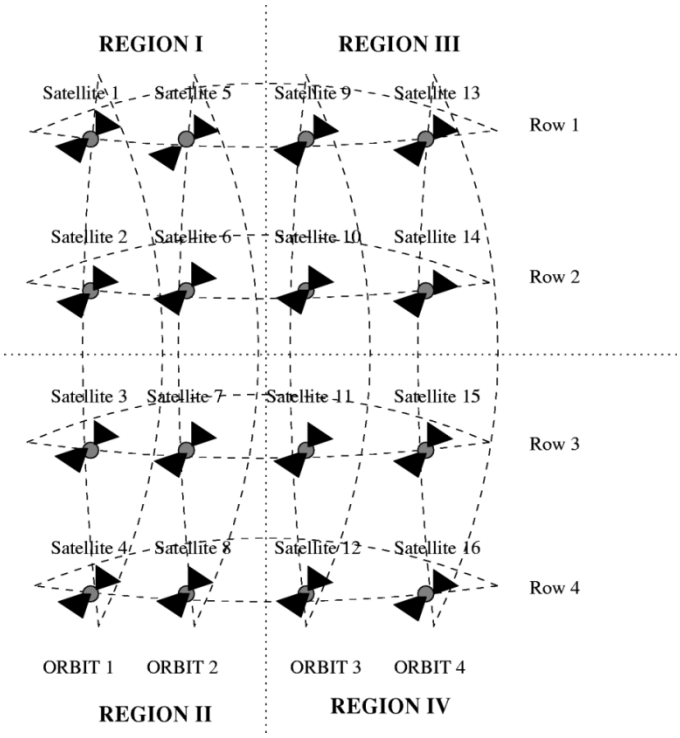

Fig. 2. Sixteen-satellite constellation.

Once the value of the normalizing constant is obtained, we can compute blocking probabilities by summing up all the appropriate blocking states. Consider the three-satellite orbit of Fig. 1. The probability that a call that either originates or terminates at satellite 1 will be blocked on the UDL of that satellite is given by

$$P_{\mathrm{UDL}_1} = \sum_{2n_{11}+n_{12}+n_{13}=C_{\mathrm{UDL}}} P(\underline{n}) \tag{12}$$

while the probability that a call originating at satellite i (or satellite j) and terminating at satellite j (or i) will be blocked by the intersatellite link (i, j) is

$$P_{\mathrm{ISL_{ij}}} = \begin{cases} 0, & C_{\mathrm{ISL}} > C_{\mathrm{UDL}} \\ \displaystyle\sum_{n_{ij}=C_{\mathrm{ISL}}} P(\underline{n}), & \text{otherwise.} \end{cases} \tag{13}$$

Once the blocking probabilities on all UDL and intersatellite links have been obtained using expressions similar to (12) and (13), the blocking probability of calls between any two satellites can be obtained easily.

Let k be the number of satellites in a single orbit and N be the number of random variables in the state description of the corresponding Markov process $N = k(k+1)/2$. Using the method described in [11], we can compute the normalizing constant G in time $O(C^{N-k})$ as opposed to time $O(C^N)$ needed by a brute force enumeration of all states. Although the *improvement* in the running time provided by our method for computing G increases with k, the value of N will dominate for large values of k. Numerical experiments with the above algorithm indicate that this method is limited to $k = 5$ satellites. That is, it takes an amount of time in the order of a few minutes to compute the normalizing constant G for five satellites. Thus, a different method is needed for analyzing realistic constellations of LEO satellites.

III. A Decomposition Algorithm for LEO Satellite Constellations

We now present a decomposition method for calculating call-blocking probabilities in a constellation of satellites. The constellation is decomposed into a series of subsystems, each consisting of at most three satellites. Each subsystem is analyzed separately using the exact solution described in the previous section. The results obtained from the subsystems are then combined together using an iterative scheme in order to obtain a solution to the constellation as a whole. This decomposition algorithm is a nontrivial extension of the one presented in [11] for satellites arranged in a single orbit, where there are no interorbit links.

As in the previous section, we will assume for the moment that the constellation of satellites is fixed over the earth, as in the case of geostationary satellites. That is, calls are not handed off from one satellite to another and the call-blocking probability due to handoffs is zero. Therefore, the decomposition algorithm presented in this section can only calculate the call-blocking probabilities of new calls. In the following section, we extend the algorithm to also calculate the call-blocking probabilities due to handoffs.

In order to explain how the decomposition algorithm works, let us consider a 16-satellite constellation with 4 orbits and 4 satellites per orbit, as shown in Fig. 2. In the configuration of satellites that we study, we do not take into account the presence of the seam or the fact that satellites near the north and south pole have some of their links shut down. These two cases can be taken into account by simply changing the routing paths between pairs of satellites that are affected by the lack of links over the seam and near the poles.

The constellation is fixed over the earth and we assume that each satellite in the first row has an intraplane ISL to the satellite on the same orbit located in the bottom row. For instance, satellite 1 communicates with satellite 4 via an intraplane ISL. Likewise, satellites 5 and 8 are connected by an intraplane ISL and so on. Also, each satellite in the first column communicates via an interplane ISL with the satellite on the fourth column that is located on the same row. For instance, satellite 1 has an interplane link to satellite 13 and so on.

For the purposes of our decomposition algorithm, each orbit is divided into two subsystems (shown in Fig. 3). For instance, orbit 1 is divided into subsystem 1, consisting of satellites 1 and 2, and subsystem 2, consisting of satellites 3 and 4. Orbit 2 is divided into subsystem 3, consisting of satellites 5 and 6, and subsystem 4, consisting of satellites 7 and 8; likewise for orbits 3 and 4. Similarly, each row of four satellites in Fig. 2 is divided into two subsystems. The 16-satellite constellation is, thus, divided into 16 subsystems as shown in Fig. 3.

In order to analyze subsystem 1 in isolation, we need to have some information from other subsystems. Specifically, we need to know the probability that a call originating at a satellite in subsystem 1 and terminating at a satellite in subsystem r, where $r > 1$, will be blocked due to lack of capacity in a link of any subsystem that it has to traverse, including subsystem r.

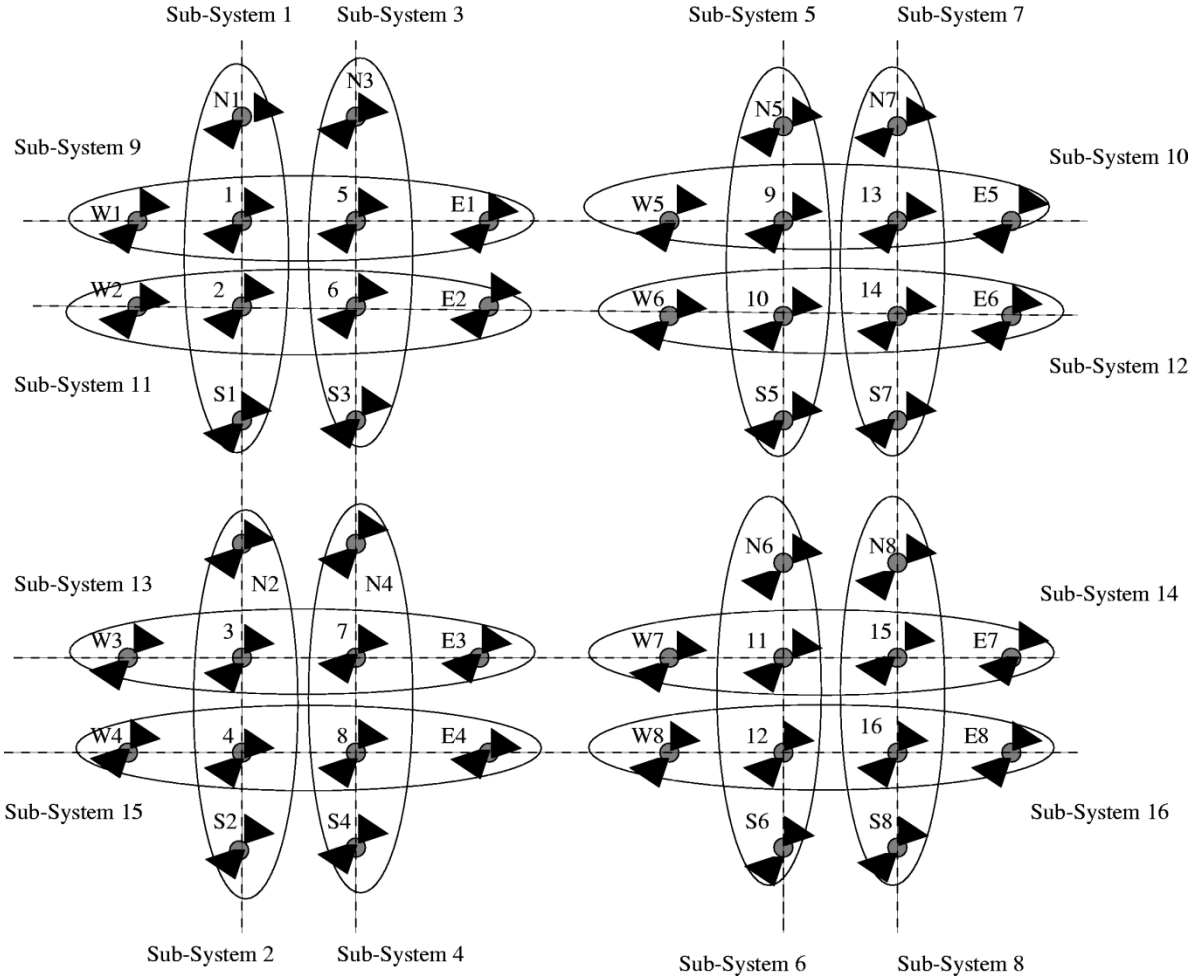

Fig. 3. Augmented subsystems for constellation of Fig. 2.

Also, we need to know the number of calls that originate at other subsystems and terminate in subsystem 1. Similar information is needed in order to analyze any other subsystem.

In view of this, each subsystem within an orbit is augmented to include two fictitious satellites, referred to as N and S. These two satellites are used to represent the aggregate traffic generated by other satellites, which flows into (or out of) the subsystem along links north or south of the subsystem, respectively. For instance, subsystem 1, shown in Fig. 3, is augmented with fictitious satellites $N1$ and $S1$. A call originating at satellite i, $i = 1, 2$ and terminating at satellite j, $j = 3, 4$ are represented in our subsystem by a call from satellite i to one of the fictitious satellites $N1$ or $S1$. Depending upon i and j, this call may be routed differently. In our augmented subsystem, a call will be routed to $S1$ if the shortest-path route passes through satellites south of the subsystem. A call will be routed to $N1$ if the shortest-path route goes toward the north.[2] In other words, satellite $N1$ (respectively, $S1$) in the augmented subsystem is the destination satellite for all calls that originate in satellite i of subsystem 1 and are routed to satellite j, located outside that subsystem in the clockwise (respectively, counterclockwise) direction.

[2]We note again that the algorithm can handle any fixed-routing scheme in addition to the shortest-path scheme.

This augmented subsystem captures the traffic outside the subsystem that travels on the same orbit, i.e., on intraplane ISLs. In addition, we also have to consider traffic that uses interplane ISLs. For instance, let us consider again subsystem 1. A call originating at satellite 1 and terminating at satellite 6 will use the intraplane ISL to satellite 2 and then the interplane ISL between satellites 2 and 6. In order to account for traffic-traversing interplane ISLs, we also decompose each row of satellites into two subsystems, each consisting of two satellites. For instance, the first row of satellites is divided into subsystem 9, consisting of satellites 1 and 5, and subsystem 10, consisting of satellites 9 and 13. The 16-satellite constellation is, thus, divided into an additional eight subsystems, as shown in Fig. 3. Each subsystem is augmented to include two fictitious satellites, referred to as E and W. As before, the fictitious E and W satellites are used to represent the aggregate traffic generated by other satellites, which flows into (or out of) the subsystem along links east or west of the subsystem, respectively. For instance, a call originating at, say, satellite $i, i = 1, 5$ and terminating at satellite j, $j = 9, 13$ will be represented in our subsystem 9 as a call from i to either $E1$ or $W1$, depending upon the shortest-path route of the call. As another example, consider a call between satellites 5 and 11. Using shortest-path routing, this call is routed through satellites 9 and 10. Within the augmented subsystem 9, this par-

ticular is represented as a call between satellite 5 and fictitious satellite $E1$.

In order to analyze the augmented subsystems in Fig. 3, we introduce the *effective* arrival rates $\hat{\lambda}_{ij}$, including rates $\hat{\lambda}_{i,N}$, $\hat{\lambda}_{i,S}$ (or $\hat{\lambda}_{i,E}$, $\hat{\lambda}_{i,W}$) within each subsystem. The effective rate $\hat{\lambda}_{ij}$ captures the rate of calls between satellite i and satellite j, *as seen from within this subsystem*. In particular, the effective rate $\hat{\lambda}_{i,N}$ (or any other rate involving any of the other fictitious satellites S, E, or W) captures the rate of calls originating at satellite i and leaving the subsystem over an ISL that goes through the fictitious satellite N.

Based on this decomposition, computing the blocking probability of a call depends on whether or not the originating and terminating satellites of the call are within the same subsystem. In the former case, the blocking probability is computed directly as a byproduct of solving the subsystem in isolation. In the latter case, the blocking probability is computed by taking into account all the subsystems in the call's path. Returning to Fig. 3, a call originating at satellite 1 and terminating at satellite 6 will be analyzed in two steps. At the first step, it is a call within subsystem 1 between satellites 1 and 2. This call then leaves this subsystem from satellite 2 and is analyzed using subsystem 11. From the point of view of subsystem 11, this is a call between satellites 2 and 6. As another example, analyzing a call between satellite 1 and satellite 8 involves three subsystems. Within subsystem 1, it is viewed as a call between satellite 1 and (fictitious) satellite $N1$. In subsystem 2, it is considered a call between (fictitious) satellite $S2$ and satellite 4. Finally, in subsystem 15, it is a call between satellites 4 and 8.

For a step-by-step precise description of the iterative algorithm, including pseudocode, the reader is referred to [12]. We now illustrate the decomposition algorithm using the 16-satellite constellation shown in Fig. 3. Initially, we solve subsystem 1 in isolation. This system in isolation is described by the following Markov process:

$$\underline{n} = (n_{11}, n_{12}, n_{1N_1}, n_{1S_1}, n_{22}, n_{2N_1}, n_{2S_1}). \tag{14}$$

We solve subsystem 1 exactly by using the approach described in the previous section. The arrival rates used in the solution are the effective arrival rates obtained using expressions (15)–(21). We now explain expression (15) for effective rate $\hat{\lambda}_{1,N1}$ in more detail. Expressions (16)–(21), as well as expressions for the other subsystems not shown here, are obtained in a similar fashion. Note that, in these expressions, quantities p_{ij} represent the probability that a call between two satellites traveling through the path segment (i, j) in another subsystem will be blocked due to the lack of capacity in that segment.

Consider expression (15) for effective rate $\hat{\lambda}_{1,N1}$, which represents the rate of calls originating at satellite 1 and leaving the subsystem over ISL 1-4 in Fig. 2. Because of the shortest-path routing we consider here, these are calls terminating at satellites 4, 8, 12, and 16. Consequently, the right-hand side of (15) consists of four terms, one for calls terminating at each of these four satellites. The first term in (15), $(1-p_{4,S_2})\lambda_{1,4}$, represents the effective arrival rate of calls between satellites 1 and 4, as seen by subsystem 1. This effective rate represents the fraction of calls between satellites 1 and 4 not blocked in subsystem 2 between satellites 4 and S_2 and is given by the product of the arrival rate $\lambda_{1,4}$ of new calls between satellites 1 and 4 times the probability that a call is not blocked between satellite 4 and (fictitious) satellite $S2$) in subsystem 2. The second term is obtained similarly by accounting for all the subsystems in the shortest path between satellites 1 and 8. A call between satellites 1 and 8 may be blocked either in subsystem 2, between satellites 4 and S_2, or in subsystem 15, between satellites 4 and 8. Therefore, the effective arrival rate for a call between satellites 1 and 8 as seen by subsystem 1 is $(1-p_{4,S_2})(1-p_{4,8})\lambda_{1,8}$. This expression gives us the proportion of calls that are not blocked in subsystems 2 and 15. The third term, $(1-p_{4,S_2})(1-p_{4,8})(1-p_{W_8,12})\lambda_{1,12}$, provides the effective arrival rate between satellites 1 and 12. This expression gives us the proportion of the traffic that is not blocked between satellites 4 and S_2, 4 and 8, and W_8 and 12. The last term of $\lambda_{1,N1}$ is similar to the previous term except that it accounts for the subsystems along the shortest path to satellite 16

$$\begin{aligned}
\hat{\lambda}_{1,N1} &= (1-p_{4,S_2})\lambda_{1,4} + (1-p_{4,S_2})(1-p_{4,8})\lambda_{1,8} \\
&\quad + (1-p_{4,S_2})(1-p_{4,8})(1-p_{W_8,12})\lambda_{1,12} \\
&\quad + (1-p_{4,S_2})(1-p_{4,E_4})(1-p_{W_8,16})\lambda_{1,16} \\
\hat{\lambda}_{1,S1} &= (1-p_{N_2,3})\lambda_{1,3} + (1-p_{N_2,3})(1-p_{3,7})\lambda_{1,7} \qquad (15) \\
&\quad + (1-p_{N_2,3})(1-p_{3,E_3})(1-p_{W_7,11})\lambda_{1,11} \\
&\quad + (1-p_{N_2,3})(1-p_{3,E_3})(1-p_{W_7,15})\lambda_{1,15} \qquad (16) \\
\hat{\lambda}_{1,1} &= \lambda_{1,1} \qquad (17) \\
\hat{\lambda}_{1,2} &= \lambda_{1,2} + (1-p_{2,S_1})(1-p_{N_2,3})\lambda_{1,3} + (1-p_{2,6})\lambda_{1,6} \\
&\quad + (1-p_{2,S_1})(1-p_{N_2,3})(1-p_{3,7})\lambda_{1,7} \\
&\quad + (1-p_{2,E_2})(1-p_{W_6,10})\lambda_{1,10} \\
&\quad + (1-p_{2,S_1})(1-p_{N_2,3}) \\
&\quad \times (1-p_{3,E_3})(1-p_{W_7,11})\lambda_{1,11} \\
&\quad + (1-p_{2,W_2})(1-p_{E_6,14})\lambda_{1,14} \\
&\quad + (1-p_{2,S_1})(1-p_{N_2,3}) \\
&\quad \times (1-p_{3,W_3})(1-p_{E_7,15})\lambda_{1,15} \\
&\quad + (1-p_{1,N_1})(1-p_{S_2,4})\lambda_{2,4} + (1-p_{1,5})\lambda_{2,5} \\
&\quad + (1-p_{1,N_1})(1-p_{S_2,4})(1-p_{4,8})\lambda_{2,8} \\
&\quad + (1-p_{1,E_1})(1-p_{W_5,9})\lambda_{2,9} \\
&\quad + (1-p_{1,N_1})(1-p_{S_2,4}) \\
&\quad \times (1-p_{4,E_4})(1-p_{W_8,12})\lambda_{2,12} \\
&\quad + (1-p_{1,W_1})(1-p_{E_5,13})\lambda_{2,13} \\
&\quad + (1-p_{1,N_1})(1-p_{S_2,4}) \\
&\quad \times (1-p_{4,W_4})(1-p_{E_8,16})\lambda_{2,16} \qquad (18) \\
\hat{\lambda}_{2,2} &= \lambda_{2,2} \qquad (19) \\
\hat{\lambda}_{2,N1} &= (1-p_{4,S_2})\lambda_{2,4} + (1-p_{4,S_2})(1-p_{4,8})\lambda_{2,8} \\
&\quad + (1-p_{4,S_2})(1-p_{4,E_4})(1-p_{W_8,12})\lambda_{2,12} \\
&\quad + (1-p_{4,S_2})(1-p_{4,W_4})(1-p_{E_8,16})\lambda_{2,16} \qquad (20) \\
\hat{\lambda}_{2,S1} &= (1-p_{3,N_2})\lambda_{2,3} + (1-p_{3,N_2})(1-p_{3,7})\lambda_{2,7} \\
&\quad + (1-p_{3,N_2})(1-p_{3,E_3})(1-p_{W_7,11})\lambda_{2,11} \\
&\quad + (1-p_{3,N_2})(1-p_{3,W_3})(1-p_{E_7,15})\lambda_{2,15}. \qquad (21)
\end{aligned}$$

Equations (15)–(21) are used to solve subsystem 1. Similar equations, not shown here, are used to solve the other subsystems in isolation. The values of quantities p_{ij} are updated at each iteration and represent our best estimate for the value of the corresponding blocking probability at the beginning of the iteration. For the first iteration, we use $p_{ij}^{(0)} = 0$ for all i and j. During the hth iteration, each subsystem is solved in isolation using the blocking probabilities $p_{ij}^{(h-1)}$ computed during the previous iteration. As a result of the solution to the subsystem, a new set of values $p_{ij}^{(h)}$ for the blocking probabilities are obtained, which are used in the next iteration. This iterative procedure continues until the blocking probabilities converge.

Once the iterative procedure terminates, the blocking probability between any two satellites can be computed as follows. If both satellites are in the same subsystem, the corresponding blocking probability is readily available as part of the last solution to the subsystem. For example, the blocking probability between satellite 1 and satellite 2, both of which are in subsystem 1, is given by the value of $p_{1,2}$, obtained by the solution to this subsystem. However, the blocking probability from satellite 1 to satellite 12 in subsystem 6 is given by

$$P_{1,12} = 1 - \big((1-p_{1,1})(1-p_{1,N1})(1-p_{4,S2})(1-p_{8,E4}) \times (1-p_{4,8})(1-p_{W8,12})(1-p_{12,12})\big). \quad (22)$$

In the above expression, the overall blocking probability is obtained by simply multiplying the blocking probabilities at each subsystem along the path between satellites 1 and 12. The first and last terms, $(1-p_{1,1})$ and $(1-p_{12,12})$, respectively, represent the blocking probability at UDL. The remaining terms represent the blocking probability at intersatellite links.

Any constellation with a large number of satellites can be decomposed in a similar manner, into a number of subsystems, each consisting of three or fewer satellites. The decomposition method is similar to the one above in that for subsystem r, the remaining satellites are aggregated to two fictitious satellites. Each subsystem is analyzed in succession as described above. We note that when employing the decomposition algorithm, the selection of the subsystem size will depend on the number of satellites in the original orbit and how efficiently we can calculate the exact solution of the Markov process associated with each subsystem. It is well known in decomposition algorithms that the larger the individual subsystems that have to be analyzed in isolation, the better the accuracy of the decomposition algorithm. Thus, as we mentioned above, we have decided to decompose a constellation into subsystems of the largest size (three of the original satellites plus two fictitious ones) for which we can efficiently analyze the Markov process.

IV. Modeling Handoffs

So far, we have assumed that the constellation is fixed over the earth. In this section, we remove this assumption and we let the satellites travel along their orbits. Below, we first consider the relatively straightforward case of the earth-fixed coverage. We then examine the more involved case of satellite-fixed coverage.

A. Earth-Fixed Coverage

Let us now turn to the problem of determining blocking probabilities in a LEO satellite constellation with earth-fixed coverage. Let L denote the number of orbits and S the number of satellites in each orbit. In this case, we assume that the earth is divided into S fixed cells (footprints) along L streets of coverage and that time is divided in intervals of length T such that, during a given interval, each satellite serves a certain cell by continuously redirecting its beams. At the end of each interval, i.e., every T time units, all satellites simultaneously redirect their beams to serve the next footprint along their orbit. They also hand off currently served calls to the next satellite in the orbit.

We make the following observations about this system. Handoff events are periodic with a period of T time units and handoffs take place in bulk at the end of each period. Also, there is no call blocking due to handoffs since, at each handoff event, a satellite passes its calls to the one following it and simply inherits the calls of the satellite ahead of it. Finally, within each period T, the system can be modeled as one with no handoffs, such as described in the previous subsection. Given that the period T is equal to the orbit period (approximately 100 minutes) divided by the number of satellites at each orbit, we can assume that the system reaches steady state within the period and, thus, the initial conditions (i.e., the number of calls inherited by each satellite at the beginning of the period) do not affect its behavior.

Now, since every T unit of time each satellite assumes the traffic carried by the satellite ahead, from the point of view of an observer on the earth, this system appears to be as if the satellites are permanently fixed over their footprints. Hence, we can use the decomposition algorithm presented above to analyze this system.

B. Satellite-Fixed Coverage

Consider now satellite fixed-cell coverage. As a satellite moves, its footprint on the earth (the cell served by the satellite) also moves with it. As customers move out of the footprint area of a satellite, their calls are handed off to the satellite following it from behind. In order to model handoffs in this case, we make the assumption that potential customers are uniformly distributed over the part of the earth served by the satellites in the orbit. This assumption has the following two consequences.

- The arrival rate λ of new calls to each satellite remains constant as it moves around the earth. Then, the arrival rate of calls between satellite i and satellite j is given by $\lambda_{ij} = \lambda r_{ij}$ where r_{ij} is the probability that a call originating by a customer served by satellite i is for a customer served by satellite j.
- The active customers served by a satellite can be assumed to be uniformly distributed over the satellite's footprint. As a result, the rate of handoffs from satellite i to satellite j, which is following from behind, is proportional to the number of calls at satellite i.

Clearly, the assumption that customers are uniformly distributed (even within an orbit) is an approximation.

Let A denote the area of a satellite's footprint and v denote a satellite's speed. As a satellite moves around the earth within a time interval of length Δt, its footprint will move a distance

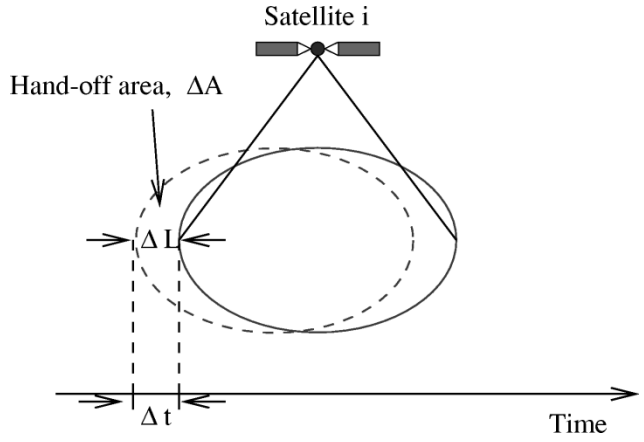

Fig. 4. Calculation of the handoff probability.

of ΔL, as shown in Fig. 4. Calls involving customers located in the part of the original footprint of area ΔA (the handoff area), which is no longer served by the satellite, are handed off to the satellite following it. Let $\Delta A = A\beta\Delta L$, where β depends on the shape of the footprint. Because of the assumption that active customers are uniformly distributed over the satellite's footprint, the probability q that a customer will be handed off to the next satellite along the sky within a time interval of length Δt is

$$q = \frac{\Delta A}{A} = \beta \Delta L = \beta v \Delta t. \tag{23}$$

Define $\alpha = \beta v$. Then, when there are n customers served by a satellite, the *rate* of handoffs to the satellite following it will be αn.

1) Single Subsystem: Let us first return to the three-satellite orbit (see Fig. 1) and introduce handoffs. This system can be described by a continuous-time Markov process with the same number of random variables as the no-handoffs model of Section II (i.e., $n_{11}, \ldots, n_{33}$), the same transition rates (2) and (3), but with a number of additional transition rates to account for handoffs. We will now derive the transition rates due to handoffs.

Consider calls between a customer served by satellite 1 and a customer served by satellite 2. There are n_{12} such calls serving $2n_{12}$ customers: n_{12} customers on the footprint of satellite 1 and n_{12} on the footprint of satellite 2. Consider a call between customer A and customer B, served by satellites 1 and 2, respectively. The probability that customer A will be in the handoff area of satellite 1 but B will not be in the handoff area of satellite 2 is $q(1-q) = q - q^2$. From (23), we have that $\lim_{\Delta t \to 0}(q^2/\Delta t) = 0$, so the rate at which these calls experience a handoff from satellite 1 to satellite 3 that follows it is αn_{12}. Based on the above discussion, we have

$$r(\underline{n}, \underline{n} - \underline{1}_{12} + \underline{1}_{23}) = \alpha n_{12}, \qquad n_{12} > 0. \tag{24}$$

Similarly, the probability that customer B will be in the handoff area of satellite 2 but A will not be in the handoff area of satellite 1 is $q(1-q) = q - q^2$. Thus, the rate at which these calls experience a handoff from satellite 2 to satellite 1 that follows it is again αn_{12}

$$r(\underline{n}, \underline{n} - \underline{1}_{12} + \underline{1}_{11}) = \alpha n_{12}, \qquad n_{12} > 0. \tag{25}$$

On the other hand, the probability that both customers A and B are in the handoff area of their respective satellites is q^2, which, from (23), is $o(\Delta t)$ and, thus, simultaneous handoffs are not allowed.

Now consider calls between customers that are both served by the same satellite, say, satellite 1. There are n_{11} such calls serving $2n_{11}$ customers. The probability that exactly one of the customers of a call is in the handoff area of satellite 1 is $2q(1-q)$, so the rate at which these calls experience handoffs (involving a single customer) to satellite 3 is $2\alpha n_{11}$

$$r(\underline{n}, \underline{n} - \underline{1}_{11} + \underline{1}_{13}) = 2\alpha n_{11}, \qquad n_{11} > 0. \tag{26}$$

As before, the probability that both customers of the call are in the handoff area of satellite 1 is q^2 and, again, no simultaneous handoffs are allowed.

The transition rates involving the other four random variables in the state description (1) can be derived using similar arguments. For completeness, these transition rates are provided in (27)–(32)

$$r(\underline{n}, \underline{n} - \underline{1}_{13} + \underline{1}_{12}) = \alpha n_{13}, \qquad n_{13} > 0 \tag{27}$$
$$r(\underline{n}, \underline{n} - \underline{1}_{13} + \underline{1}_{33}) = \alpha n_{13}, \qquad n_{13} > 0 \tag{28}$$
$$r(\underline{n}, \underline{n} - \underline{1}_{22} + \underline{1}_{12}) = 2\alpha n_{22}, \qquad n_{22} > 0 \tag{29}$$
$$r(\underline{n}, \underline{n} - \underline{1}_{23} + \underline{1}_{13}) = \alpha n_{23}, \qquad n_{23} > 0 \tag{30}$$
$$r(\underline{n}, \underline{n} - \underline{1}_{23} + \underline{1}_{22}) = \alpha n_{23}, \qquad n_{23} > 0 \tag{31}$$
$$r(\underline{n}, \underline{n} - \underline{1}_{33} + \underline{1}_{23}) = 2\alpha n_{33}, \qquad n_{33} > 0. \tag{32}$$

From the queueing point of view, this system is a queueing network of *M/M/K/K* queues as described in Section II, where customers are allowed to move between queues according to (24)–(32). (Recall that in the queueing model of Section II, customers are not allowed to move from node to node.) This queueing network has a product–form solution similar to (10). Let γ_{ij} denote the total arrival rate of calls between satellites i and j, including new calls (arriving at a rate of λ_{ij}) and handoff calls (arriving at an appropriate rate). The values of γ_{ij} can be obtained by solving the traffic equations for the queueing network. Let also $\nu_{ij} n_{ij}$ be the departure rate when there are n_{ij} of these calls, including call termination (at a rate of $\mu_{ij} n_{ij}$) and call handoff (at a rate of $2\alpha n_{ij}$). Also, define $\rho'_{ij} = \gamma_{ij}/\nu_{ij}$. Then, the solution for this queueing network is given by

$$\begin{aligned} P(\underline{n}) &= P(n_{11}, n_{12}, n_{13}, n_{22}, n_{23}, n_{33}) \\ &= \frac{1}{G} \times \frac{(\rho'_{11})^{n_{11}}}{n_{11}!} \frac{(\rho'_{12})^{n_{12}}}{n_{12}!} \frac{(\rho'_{13})^{n_{13}}}{n_{13}!} \frac{(\rho'_{22})^{n_{22}}}{n_{22}!} \\ &\quad \times \frac{(\rho'_{23})^{n_{23}}}{n_{23}!} \frac{(\rho'_{33})^{n_{33}}}{n_{33}!} \end{aligned} \tag{33}$$

which is identical to (10) except that ρ_{ij} has been replaced by ρ'_{ij}. Therefore, the exact solution we presented in Section II is directly applicable to this new queueing network as well.

2) Constellation of Satellites: To analyze a constellation of satellites with handoffs, we use the same decomposition algorithm presented in Section III. The main difference is that instead of using the arrival and departure rates for new calls λ_{ij} and μ_{ij}, respectively, we use the rates γ_{ij} and ν_{ij}, which account for both new and handoff calls. The latter are obtained by solving the traffic equations for the queueing networks. Therefore, our analysis of a satellite constellation is shown in the following steps.

1) The constellation is modeled as a queueing network of *M/M/K/K* queues, where each queue represents the number of calls between a pair of satellites (i, j) (no handoffs case). A number of constraints, similar to (4)–(9), are imposed in the state space to account for the fact that some calls share common links.

2) Based the discussion in the previous section, in order to model handoffs, we introduce additional transitions of customers moving from one queue to another.

3) We solve exactly the traffic equations of the queueing network resulting from Step 2) to obtain the new arrival rates.

4) We apply the decomposition algorithm described in Section III by using the arrival rates from Step 3.

Unfortunately, solving the traffic equations for the constellation as a whole is computationally expensive, since it takes time $O(N^3)$, where N is the number of states in the Markov process for the whole constellation. The number N of states, in turn, is exponential in the number K of satellites in the constellation. In order to decrease the complexity of the process, in the next section we develop an approximate solution for the traffic equations.

3) A Distributed Solution for Traffic Equations: Instead of defining the traffic equations for the whole system, we use a distributed approach. That is, we treat each subsystem defined in Section III separately and we solve the traffic equations for each subsystem in isolation. Transitions between subsystems are also taken into account.

In order to explain the distributed algorithm, we refer to Fig. 3. Let us consider subsystem 1 in isolation. Recall that this subsystem is described by the Markov process defined in (14). Consider random variable n_{12}. This random variable may represent a call originating at satellite 1 and terminating at satellite 2, a call that originates at satellite 1 (or satellite 2) and uses the ISL 1-2 but does not terminate at satellite 2 (respectively, satellite 1) or a call that simply uses ISL 1-2 but does not originate or terminate at either satellite 1 or satellite 2. Based on this observation, the transitions between states of the Markov process due to handoffs depend on the source/destination pair of a call.

First consider the case where a call originates at satellite 1 and terminates at satellite 2. If the customer under satellite 1 makes a handoff to satellite 2, this call becomes a call handled by satellite 2 alone (i.e., it both originates and terminates at satellite 2). Thus, we have the following transition:

$$r(\underline{n},\, \underline{n}-\underline{1}_{12}+\underline{1}_{22}) = \alpha n_{12}, \qquad n_{12}>0. \tag{34}$$

Another possibility is for the customer under satellite 2 to make a handoff to satellite 3 (see Fig. 2). In this case, from the point of view of subsystem 1, this call becomes a call between satellite 1 and satellite S1. Therefore, the transition is

$$r(\underline{n},\, \underline{n}-\underline{1}_{12}+\underline{1}_{1S_1}) = \alpha n_{12}, \qquad n_{12}>0. \tag{35}$$

On the other hand, consider a customer in satellite 1 with a connection to satellite 10. The call is routed through satellites 2 and 6 to satellite 10. Therefore, in subsystem 1, this is a call between satellites 1 and 2. If the customer under satellite 1 makes a handoff, the call leaves subsystem 1 and is treated by subsystem 11 after the handoff. This transition is shown in (36) as

$$r(\underline{n},\, \underline{n}-\underline{1}_{12}) = \alpha n_{12}, \qquad n_{12}>0. \tag{36}$$

The transition rates involving the other random variables in the state description (14) can be derived by using similar arguments. For completeness, these transition rates are provided in (37)–(47) as

$$r(\underline{n},\, \underline{n}-\underline{1}_{11}+\underline{1}_{12}) = 2\alpha n_{11}, \qquad n_{11}>0 \tag{37}$$
$$r(\underline{n},\, \underline{n}-\underline{1}_{1N_1}+\underline{1}_{11}) = \alpha n_{1N_1}, \qquad n_{1N_1}>0 \tag{38}$$
$$r(\underline{n},\, \underline{n}-\underline{1}_{1N_1}+\underline{1}_{2N_1}) = \alpha n_{1N_1}, \qquad n_{1N_1}>0 \tag{39}$$
$$r(\underline{n},\, \underline{n}-\underline{1}_{1N_1}) = \alpha n_{1N_1}, \qquad n_{1N_1}>0 \tag{40}$$
$$r(\underline{n},\, \underline{n}-\underline{1}_{1S_1}+\underline{1}_{1N_1}) = \alpha n_{1S_1}, \qquad n_{1S_1}>0 \tag{41}$$
$$r(\underline{n},\, \underline{n}-\underline{1}_{1S_1}+\underline{1}_{2S_1}) = \alpha n_{1S_1}, \qquad n_{1S_1}>0 \tag{42}$$
$$r(\underline{n},\, \underline{n}-\underline{1}_{1S_1}) = \alpha n_{1S_1}, \qquad n_{1S_1}>0 \tag{43}$$
$$r(\underline{n},\, \underline{n}-\underline{1}_{22}+\underline{1}_{2S_1}) = 2\alpha n_{22}, \qquad n_{22}>0 \tag{44}$$
$$r(\underline{n},\, \underline{n}-\underline{1}_{2N_1}+\underline{1}_{12}) = \alpha n_{2N_1}, \qquad n_{2N_1}>0 \tag{45}$$
$$r(\underline{n},\, \underline{n}-\underline{1}_{2N_1}) = \alpha n_{2N_1}, \qquad n_{2N_1}>0 \tag{46}$$
$$r(\underline{n},\, \underline{n}-\underline{1}_{2S_1}) = 2\alpha n_{2S_1}, \qquad n_{2S_1}>0. \tag{47}$$

Once the transition rates are known, the traffic equations for each queue can be written easily as shown in (48)–(54) as

$$\gamma_{11} = \hat{\lambda}_{1,1} + \frac{\alpha}{3\alpha+\mu}\,\gamma_{1N_1} \tag{48}$$
$$\gamma_{12} = \hat{\lambda}_{1,2} + \frac{2\alpha}{2\alpha+\mu}\,\gamma_{11} + \frac{\alpha}{2\alpha+\mu}\,\gamma_{2N_1} \tag{49}$$
$$\gamma_{1N_1} = \hat{\lambda}_{1,N_1} + \frac{\alpha}{3\alpha+\mu}\,\gamma_{1S_1} \tag{50}$$
$$\gamma_{1S_1} = \hat{\lambda}_{1,S_1} + \frac{\alpha}{3\alpha+\mu}\,\gamma_{12} \tag{51}$$
$$\gamma_{22} = \hat{\lambda}_{2,2} + \frac{\alpha}{3\alpha+\mu}\,\gamma_{12} \tag{52}$$
$$\gamma_{2N_1} = \hat{\lambda}_{2,N_1} + \frac{\alpha}{3\alpha+\mu}\,\gamma_{1N_1} \tag{53}$$
$$\gamma_{2S_1} = \hat{\lambda}_{2,S_1} + \frac{2\alpha}{2\alpha+\mu}\,\gamma_{22} + \frac{\alpha}{3\alpha+\mu}\,\gamma_{1S_1}. \tag{54}$$

The solution to the traffic equations above gives us the new $\rho'_{ij} = \gamma_{ij}/\nu_{ij}$ At each iteration, after calculating the new *effective* arrival rates $\{\hat{\lambda}_{ij}\}$, we compute new $\{\gamma_{ij}\}$ using expressions (48)–(54) and from these $\{\gamma_{ij}\}$ we obtain new $\{\rho'_{ij}\}$. This procedure repeats for each subsystem until the blocking probabilities converge. Since each subsystem has a small, fixed number of satellites, solving the traffic equations (48)–(54) for a single subsystem takes constant time. At each iteration, the time needed to solve the traffic equations is proportional to the

number of subsystems, which, in turn, is linear in the number K of satellites in the constellation. Consequently, this distributed approach to solving the traffic equations results in substantial savings in terms of computation compared to directly solving the traffic equations for the whole constellation, which takes time exponential in K.

V. Bounds on the Link Blocking Probabilities

We now show how to obtain lower and upper bounds on the call-blocking probabilities of a satellite constellation. Because the bounds can be computed quite efficiently, taking time that is polynomial in the number of satellites and the number of channels (capacity) of each link, they can be useful for satellite constellations of realistic size employing multiple beams per satellite. The decomposition algorithm of Section III can be applied in such systems by considering each beam as a single "satellite" serving its own (smaller) cell. In this case, however, the number of "satellites" becomes very large, in the order of thousands. In turn, the number of calls (which is quadratic in the number of satellites) and the number of subsystems in which the constellation is decomposed also increases accordingly. As a result, the decomposition algorithm may take hours to complete. On the other hand, the method developed in this section can provide bounds on the call-blocking probabilities in a very short time, in the order of minutes.

For clarity of presentation, we derive the bounds for the three-satellite orbit (i.e., a single subsystem) shown in Fig. 1 and analyzed in Section II. The bounds can be extended in a straightforward manner for a whole satellite constellation.

In this section, we develop bounds for the probability that any call using a given link ℓ (UDL or intersatellite) is blocked, i.e., that all channels of link ℓ are busy. Once upper (respectively, lower) bounds have been obtained for all links in the satellite network, upper (respectively, lower) bounds on the call-blocking probabilities can be computed by simply multiplying the upper (respectively, lower) bounds on all the links along each call's path. The approach is similar for all links; therefore, we will illustrate the bounds by considering only one link, the UDL of satellite 1 (refer to Fig. 1). From (4) we immediately have that the states $\underline{n}$ for which all the channels of the UDL of satellite 1 are busy such that $2n_{11} + n_{12} + n_{13} = C_{\text{UDL}}$.

Let us first consider the normalizing constant G, given in (11). Recall that the state space Ω includes all the states $\underline{n}$ that satisfy constraints (4)–(9). An upper bound on G can be obtained as follows:

$$G < G_u(\ell) = \left(\sum_{2n_{11}+n_{12}+n_{13} \le C_{\text{UDL}}} \frac{\rho_{11}^{n_{11}}}{n_{11}!} \frac{\rho_{12}^{n_{12}}}{n_{12}!} \frac{\rho_{13}^{n_{13}}}{n_{13}!} \right) \times \left(\sum_{\underline{n} \in \Omega | n_{11}=n_{12}=n_{13}=0} \frac{\rho_{22}^{n_{22}}}{n_{22}!} \frac{\rho_{23}^{n_{11}}}{n_{23}!} \frac{\rho_{33}^{n_{33}}}{n_{33}!} \right) \quad (55)$$

where the second sum is over all states with $n_{11} = n_{12} = n_{13} = 0$, which satisfies constraints (5)–(9). This expression is obtained by loosening the constraints (4)–(6), which correspond to the three UDL of the constellation. Specifically, we assume that the random variables corresponding to calls using a given link must satisfy the constraint on the link's capacity, but they also evolve independently of the random variables corresponding to calls using other links. The first term in parentheses corresponds to link ℓ (in this case, the UDL of satellite 1) and involves the three random variables that must obey constraint (4). The second term corresponds to all other random variables in the state description $\underline{n}$, assuming that the random variables involved in link ℓ are zero. Since we have removed some of the dependencies among the random variables, G_u is indeed an upper bound on G. Note also that the bound G_u depends on the link ℓ we are considering, which is why in the above expression we have written G_u as a function of ℓ.

Let

$$G_0(\ell) = \sum_{\underline{n} \in \Omega | n_{11}=n_{12}=n_{13}=0} \frac{\rho_{22}^{n_{22}}}{n_{22}!} \frac{\rho_{23}^{n_{11}}}{n_{23}!} \frac{\rho_{33}^{n_{33}}}{n_{33}!}. \quad (56)$$

G_0 is the normalizing constant in a satellite system in which $n_{11} = n_{12} = n_{13} = 0$. An alternative way to view $G_0(\ell)$ is to consider a new satellite system that is identical to the original one except that there are no arrivals for any calls traversing link ℓ (i.e., $\lambda_{11} = \lambda_{12} = \lambda_{13} = 0$ in this case). Then, $G_0(\ell)$ is the normalizing constant for this new satellite system. Similarly, let

$$G_1(\ell) = \sum_{2n_{11}+n_{12}+n_{13} \le C_{\text{UDL}}} \frac{\rho_{11}^{n_{11}}}{n_{11}!} \frac{\rho_{12}^{n_{12}}}{n_{12}!} \frac{\rho_{13}^{n_{13}}}{n_{13}!} = \sum_{\underline{n} \in \Omega | n_{22}=n_{23}=n_{33}=0} \frac{\rho_{11}^{n_{11}}}{n_{11}!} \frac{\rho_{12}^{n_{12}}}{n_{12}!} \frac{\rho_{13}^{n_{13}}}{n_{13}!}. \quad (57)$$

Accordingly, $G_1(\ell)$ is the normalizing constant for a satellite system identical to the original one except that there are no arrivals for calls *not* traversing link ℓ (i.e., $\lambda_{22} = \lambda_{23} = \lambda_{33} = 0$ in this case). From (55) we obtain that

$$G < G_u(\ell) = G_1(\ell) G_0(\ell). \quad (58)$$

In the general case of a satellite constellation with K satellites, $G_u(\ell)$ for a given link ℓ can be obtained in a similar fashion. In particular, $G_u(\ell)$ for a constellation of any size is the product of two terms, where the second (respectively, first) term is the normalizing constant obtained by setting the random variables of all calls traversing (respectively, not traversing) link ℓ to zero.

Consider now the following set of blocking states for link ℓ

$$\Omega_b(\ell) = \{\underline{n} \in \Omega \mid 2n_{11} + n_{12} + n_{13} = C_{\text{UDL}}\}. \quad (59)$$

Let $B(\ell)$ denote the sum of probabilities of all blocking states

$$B(\ell) = \sum_{\underline{n} \in \Omega_b(\ell)} \frac{\rho_{11}^{n_{11}}}{n_{11}!} \frac{\rho_{12}^{n_{12}}}{n_{12}!} \frac{\rho_{13}^{n_{13}}}{n_{13}!} \frac{\rho_{22}^{n_{22}}}{n_{22}!} \frac{\rho_{23}^{n_{23}}}{n_{23}!} \frac{\rho_{33}^{n_{33}}}{n_{33}!}. \quad (60)$$

Using arguments similar to the ones used in deriving (55), we have that

$$B(\ell) < B_u(\ell) = \left(\sum_{2n_{11}+n_{12}+n_{13} = C_{\text{UDL}}} \frac{\rho_{11}^{n_{11}}}{n_{11}!} \frac{\rho_{12}^{n_{12}}}{n_{12}!} \frac{\rho_{13}^{n_{13}}}{n_{13}!} \right) G_0(\ell) = B_1(\ell) G_0(\ell) \quad (61)$$

where $B_1(\ell)$ is the sum of the blocking states in a new satellite system where only the random variables involved in link ℓ are nonzero.

From (58), we can write for a lower bound on the normalizing constant G

$$G \geq G_l(\ell) = \Delta G_1(\ell) G_0(\ell) \tag{62}$$

where $0 \leq \Delta \leq 1$. Similarly, because of (61) and for some $0 \leq \delta \leq 1$, we have that:

$$B(\ell) \geq B_l(\ell) = \delta B_1(\ell) G_0(\ell). \tag{63}$$

Let $P_b(\ell)$ denote the probability that any call using link ℓ will be blocked $P_b(\ell) = B(\ell)/G$. From (61) and (62) we obtain

$$P_b(\ell) = \frac{B(\ell)}{G} \leq \frac{B_1(\ell) G_0(\ell)}{\Delta G_1(\ell) G_0(\ell)} = \frac{1}{\Delta} \frac{B_1(\ell)}{G_1(\ell)}. \tag{64}$$

Similarly, from (63) and (58) we have that

$$P_b(\ell) = \frac{B(\ell)}{G} \geq \frac{\delta B_1(\ell) G_0(\ell)}{G_1(\ell) G_0(\ell)} = \delta \frac{B_1(\ell)}{G_1(\ell)}. \tag{65}$$

Let

$$P_{b,1}(\ell) = \frac{B_1(\ell)}{G_1(\ell)}. \tag{66}$$

Note that $P_{b,1}(\ell)$ represents the blocking probability in the satellite system where all the random variables not involved in link ℓ are set to zero. We can now rewrite $G_1(\ell)$ as follows:

$$\begin{aligned} G_1(\ell) &= \sum_{m=0}^{C_{\mathrm{UDL}}} \left(\sum_{2n_{11}+n_{12}+n_{13}=m} \frac{\rho_{11}^{n_{11}}}{n_{11}!} \frac{\rho_{12}^{n_{12}}}{n_{12}!} \frac{\rho_{13}^{n_{13}}}{n_{13}!} \right) \\ &= \sum_{m=0}^{C_{\mathrm{UDL}}} \left(\sum_{n_{11}=0}^{m/2} \frac{\rho_{11}^{n_{11}}}{n_{11}!} \left[\sum_{n_{12}+n_{13}=m-2n_{11}} \frac{\rho_{12}^{n_{12}}}{n_{12}!} \frac{\rho_{13}^{n_{13}}}{n_{13}!} \right] \right) \\ &= \sum_{m=0}^{C_{\mathrm{UDL}}} \left(\sum_{n_{11}=0}^{m/2} \frac{\rho_{11}^{n_{11}}}{n_{11}!} \frac{(\rho_{12}+\rho_{13})^{n_{12}+n_{13}}}{(n_{12}+n_{13})!} \right) \\ &= \sum_{m=0}^{C_{\mathrm{UDL}}} \left(\sum_{n_{11}=0}^{m/2} \frac{\rho_{11}^{n_{11}}}{n_{11}!} \frac{(\rho_{12}+\rho_{13})^{m-2n_{11}}}{(m-2n_{11})!} \right) \end{aligned} \tag{67}$$

where we made use of the multinomial theorem in going from the second to the third line. $G_1(\ell)$ [and, for $m = C_{\mathrm{UDL}}$, $B_1(\ell)$] can be computed in time $O(C_{\mathrm{UDL}}^2)$ using the above expression and, thus, $P_{b,1}(\ell)$ can be computed very efficiently.

Combining (64), (65), and (66) and letting $\epsilon = \min\{\delta, \Delta\}$, we obtain

$$\epsilon \leq \frac{P_b(\ell)}{P_{b,1}(\ell)} \leq \frac{1}{\epsilon}. \tag{68}$$

Expression (68) provides lower and upper bounds on the blocking probability $P_b(\ell)$ of link ℓ in terms of the blocking probability $P_{b,1}(\ell)$ of the same link in a satellite system that is identical to the original one except that there are no arrivals for calls not using link ℓ. In other words, this latter probability is the blocking probability of link ℓ when viewed in isolation and, thus, it is readily available from (67). While the values of δ and Δ (and, therefore, ϵ) are not known, we make the observation that, as the link capacities (C_{UDL} and C_{ISL}) grow and as the number of satellites (or the number of beams per satellite) grows, both Δ and δ tend to one. To see that this is true, let us refer to the definition of Δ in (62). In that expression, we decoupled the random variables involved in link ℓ from those not involved in link ℓ. In particular, the term $G_0(\ell)$ is such that all random variables involved in link ℓ are set to zero. As the link capacities grow very large, the effect of the decoupling decreases since the actual values of the random variables that were assumed to be zero have a decreasing effect on $G_0(\ell)$. Similarly, as the number K of satellites grows large, the number of calls traversing a given link grows as $O(K)$, while the total number of calls grows as $O(K^2)$. Again, therefore, the effect of the decoupling decreases as K increases and Δ tends to one. Similar observations can be made about δ. Note that δ and Δ (and, consequently, ϵ) tend to one in precisely those situations (i.e., constellations with very large link capacities and/or very large number of satellite beams) in which one would have to resort to bounds. Thus, the bounds in expression (68) are tightest in exactly those cases in which they would be most useful. Overall, numerical results with constellations of moderate sizes and a range of several traffic patterns indicate that taking $\epsilon = 0.8$ give reasonably good bounds for the link-blocking probability.

VI. Numerical Results

In this section, we verify the accuracy of the decomposition algorithm with and without handoffs by comparing the results obtained from the decomposition algorithm to simulation results. In the figures presented, the simulation results are plotted with 95% confidence intervals estimated by the method of replications. (The confidence intervals are so narrow that they are barely visible.) The number of replications is 30, with each simulation run lasting until each source/destination pair of call has at least 15 000 arrivals. For the approximate results, the iterative decomposition algorithm terminates when all call-blocking probability values have converged within 10^{-6}.

We obtained results using three different traffic patterns. Let $r_{i,j}$ denote the probability that a call originating by a customer served by satellite i is for a customer served by satellite j. The first pattern is the *uniform* traffic pattern, that is

$$r_{i,j} = \frac{1}{K} \qquad \forall\, i, j \tag{69}$$

where K is the number of satellites. The second traffic pattern is based on the notion of *traffic locality*. Specifically, it assumes that most calls originating at a satellite i of orbit l are to users in satellites $i-1$, i, and $i+1$ of orbit l or to users in satellites i of orbits $l-1$ and $l+1$. Let r_{i_l,j_k} denote the probability that a call originating by a customer served by satellite i of orbit l is for a customer served by satellite j of orbit k. This locality pattern is such that

$$r_{i_l,j_k} = \begin{cases} 0.16, & j_k = (i-1)_l,\ i_l,\ (i+1)_l,\ i_{l-1},\ i_{l+1} \\ \dfrac{0.2}{K-5}, & j_k \neq (i-1)_l,\ i_l,\ (i+1)_l,\ i_{l-1},\ i_{l+1} \end{cases} \tag{70}$$

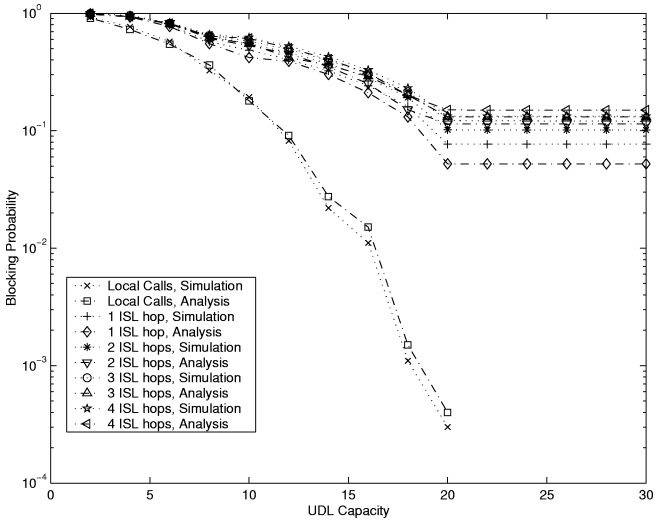

Fig. 5. Call-blocking probabilities for 16 satellites $\lambda = 5$, $C_{\rm ISL} = 10$, uniform pattern.

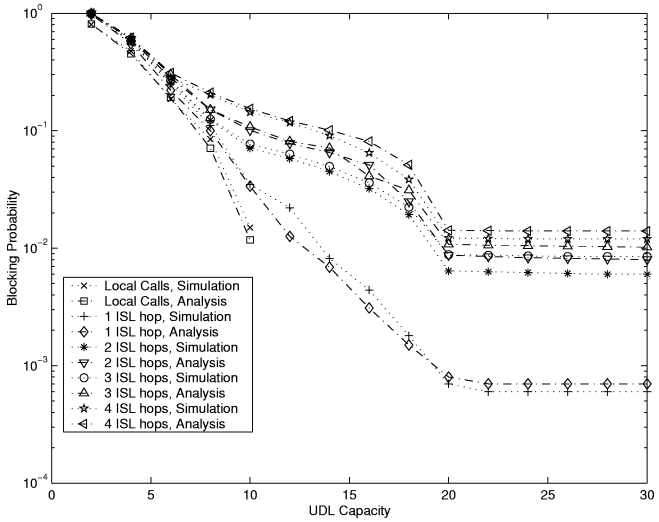

Fig. 6. Call-blocking probabilities for 16 satellites $\lambda = 2$, $C_{\rm ISL} = 10$, uniform pattern.

where addition and subtraction is modulo-k for k satellites per orbit. The third traffic pattern is a *hot-spot* pattern in which one of the satellites, satellite X, carries most of the traffic. If we let $r_{i,j}$ represent calls originating from satellite i and terminating at satellite j, then this pattern is such that

$$r_{i,j} = \begin{cases} 0.7, & i = 1, \ldots, K, j = X \\ \dfrac{0.3}{K-1}, & i, j \neq X. \end{cases} \tag{71}$$

A. The Decomposition Algorithm without Handoffs

We now verify the accuracy of the decomposition algorithm developed in Section III by comparing the blocking probabilities obtained from the algorithm to simulation results. We consider a constellation of 16 satellites with 4 orbits and 4r satellites per orbit as shown in Fig. 2. Each satellite has four ISLs; two within the same orbit and two with neighboring orbits. In this first set of tests, we assume no handoffs. In all cases studied, we have found that the algorithm converges in only a few (less than 10) iterations, taking a few minutes to terminate. On the other hand, the simulation runs of the 16-satellite system are quite expensive in terms of computation time, taking several hours to complete.

Fig. 5 plots the blocking probability against the capacity $C_{\rm UDL}$ of UDLs when the arrival rate $\lambda = 5$ and the capacity of intersatellite links $C_{\rm ISL} = 10$ for the uniform traffic pattern. Five sets of calls are shown, one for local calls (i.e., calls originating and terminating at the same satellite) and four for nonlocal calls. Each set consists of two plots, one corresponding to blocking probability values obtained by running the decomposition algorithm of Section III and one corresponding to simulation results. Each nonlocal call for which results are shown travels over a different number of intersatellite links, varying from one to four ISLs. Note that the 16-satellite constellation is such that, under shortest-path routing, the maximum number of ISLs in the path of call between any two satellites is four.

From the figure, we observe a very good agreement between the analytical results and the simulation. (Note that the y axis

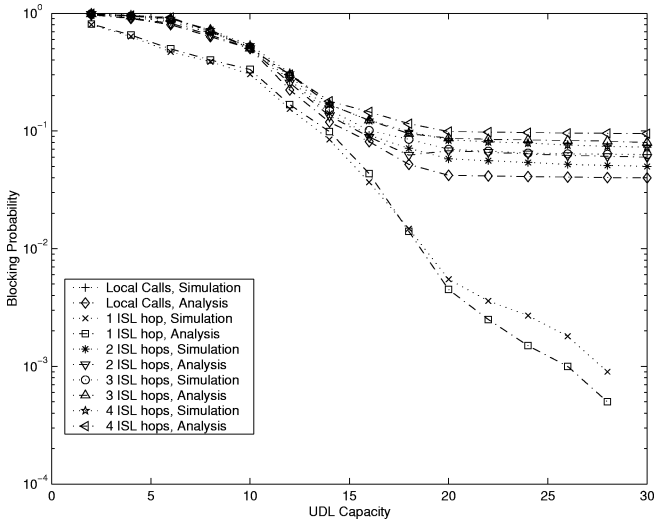

Fig. 7. Call-blocking probabilities for 16 satellites $\lambda = 5$, $C_{\rm ISL} = 10$, locality pattern.

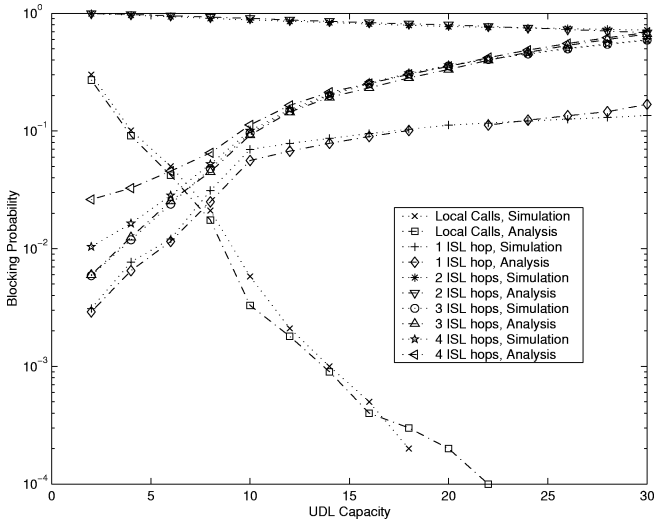

Fig. 8. Call-blocking probabilities for 16 satellites $\lambda = 5$, $C_{\rm ISL} = 10$, hot-spot pattern.

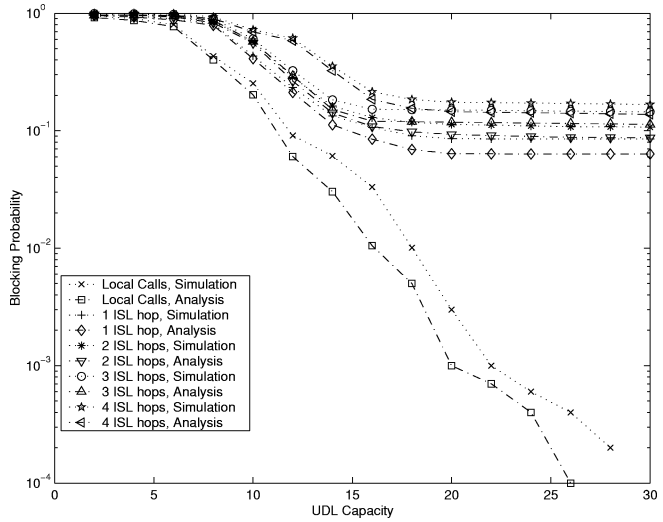

Fig. 9. Call-blocking probabilities for 16 satellites with handoff, uniform pattern.

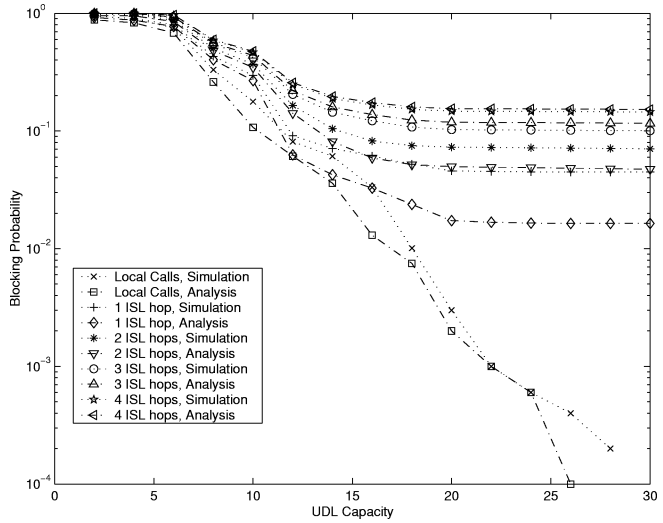

Fig. 10. Call-blocking probabilities for 16 satellites with handoff, locality pattern.

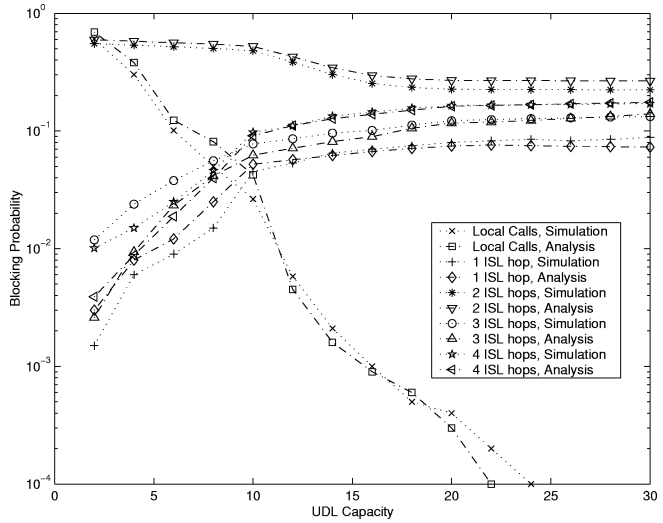

Fig. 11. Call-blocking probabilities for 16 satellites with handoff, hot-spot pattern.

uses a logarithmic scale.) The behavior of the curves can be explained by noting that, when the capacity C_{UDL} of UDLs is less than 20, these links represent a bottleneck. Thus, increasing the UDL capacity results in a significant drop in the blocking probability for all calls. When $C_{\mathrm{UDL}} > 20$, however, the intersatellite links become the bottleneck and nonlocal calls do not benefit from further increases in the UDL capacity. We also observe that the larger the number of intersatellite links over which a nonlocal call must travel, the higher its blocking probability, as expected. The blocking probability of local calls, on the other hand, drops to zero for $C_{\mathrm{UDL}} > 20$ since they do not have to compete for intersatellite links. The curves in this figure were obtained assuming that $\lambda = 5$, which results in a utilization of an ISL of around 65%. Therefore, the blocking probabilities are fairly high. In order to see the effect of a lower utilization, in Fig. 6 we plot the blocking probabilities for the same traffic pattern and the same calls when the arrival rate $\lambda = 2$ or ISL utilization of 30%.

Fig. 7 is similar to Fig. 5 but shows results for the locality traffic pattern. For the results presented we used $\lambda = 5$ and $C_{\mathrm{ISL}} = 10$ and we varied the value of C_{UDL}. We observe that the behavior of the various curves is similar to that in Fig. 5.

Finally, in Fig. 8, we observe a drastically different behavior. This scenario is the hot-spot traffic in which all satellites send most of their traffic to satellite 3. We observe that when the UDL capacity increases, the blocking probability on calls using 2 ISL hops decreases. This is due to the fact that these calls are between satellites 1 and 3. Therefore, increasing the UDL capacity on satellite 3 decreases the blocking probability of calls between satellite 1 and 3. On the other hand, the blocking probability of calls with 1, 3, and 4 ISL hops increases with increasing UDL capacity. This is due to the fact that these calls are such that their paths include one of satellite 3's ISLs. As the UDL capacity of satellite 3 increases, more calls from/to the satellite can be accepted increasing the loading on its ISLs. As a consequence, the blocking probability of calls using these ISLs also increases. Local call-blocking probabilities decrease to zero as in the previous figures.

Overall, the results in Figs. 5–8 indicate that the analytical results are in good agreement with simulation over a wide range of traffic patterns and system parameters. Thus, our decomposition algorithm can be used to study the interplay between various system parameters (e.g., C_{ISL}, C_{UDL}, traffic pattern, etc.) and their effect on the call-blocking probabilities in an efficient manner.

B. The Decomposition Algorithm with Handoffs

In this section, we verify the accuracy of the decomposition algorithm assuming handoffs. We consider the same constellation with 16 satellites. We solved the traffic equations with handoffs using the distributed approach explained in Section IV-B3. We also included handoffs in our simulation in order to test the accuracy of the algorithm.

Figs. 9–11 are similar to Figs. 5, 7, and 8, but they correspond to satellite systems with handoff calls. Specifically, the figures plot the call-blocking probability against the capacity C_{UDL} of UDLs when the arrival rate $\lambda = 5$ and the capacity of intersatellite links $C_{\mathrm{ISL}} = 10$ for the three traffic patterns we

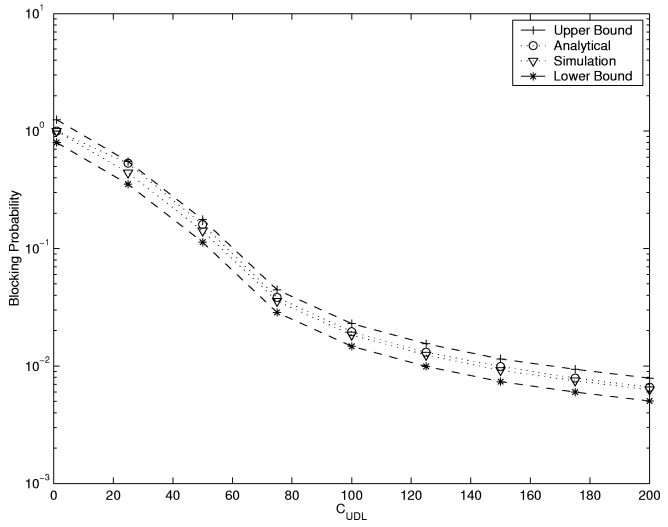

Fig. 12. Bounds, uniform pattern, $C_{\mathrm{ISL}} = 100, \lambda = 50, \epsilon = 0.8$ for bounds $\epsilon_{\min} = 0.82$.

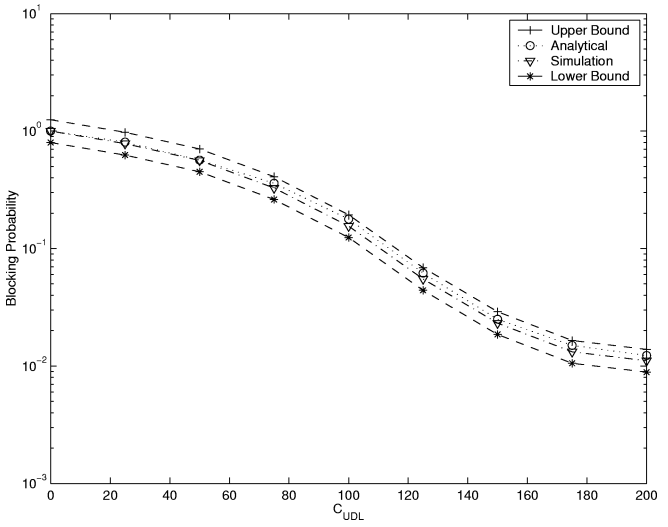

Fig. 13. Bounds, locality pattern, $C_{\mathrm{ISL}} = 100, \lambda = 50, \epsilon = 0.8$ for bounds $\epsilon_{\min} = 0.84$.

considered. As can be seen, the behavior of these plots is similar to those in the previous section. We also note that there is a good agreement between the analytical results and the simulation, although not as good as when there are no handoffs. This is expected because the calculation of the arrival rates using the distributed solution for the traffic equations introduces an additional approximation. Overall, however, the analytical curves track the simulation curves accurately, indicating that the iterative decomposition algorithm can be used to predict the call-blocking performance of a LEO satellite constellation accurately and efficiently.

C. The Upper and Lower Bounds

Figs. 12–14 demonstrate the tightness of the upper and lower bounds in expression (68) for the link-blocking probabilities derived in Section V. Each figure corresponds to one of the three traffic patterns introduced above and presents results for a 16-satellite constellation. We can rewrite (68) as follows:

$$\epsilon P_{b,\,1(\ell)} \leq P_b(\ell) \leq \frac{1}{\epsilon} P_{b,\,1(\ell)}. \tag{72}$$

Figs. 12–14 plot the following four quantities for some link ℓ against the link capacity:

1) $P_b(\ell)$, the link-blocking probability obtained through simulation;

2) $P_{b,\,1}(\ell)$, the link-blocking probability when all random variables not involved in link ℓ are set to zero; this quantity is obtained analytically in an efficient manner, as explained in Section V;

3) the lower bound $\epsilon P_{b,\,1(\ell)}$, for $\epsilon = 0.8$; and

4) the upper bound $(1/\epsilon) P_{b,\,1(\ell)}$, also for $\epsilon = 0.8$.

For each figure, we also provide the minimum ϵ for which expression (72) holds for all points plotted, which was found to be always greater than 0.8.

From the figures, we observe that using $\epsilon = 0.8$ in expression (72) provides a good approximation to the link-blocking probability $P_b(\ell)$. Most importantly, ignoring the random variables not involved with a given link results in a very efficient

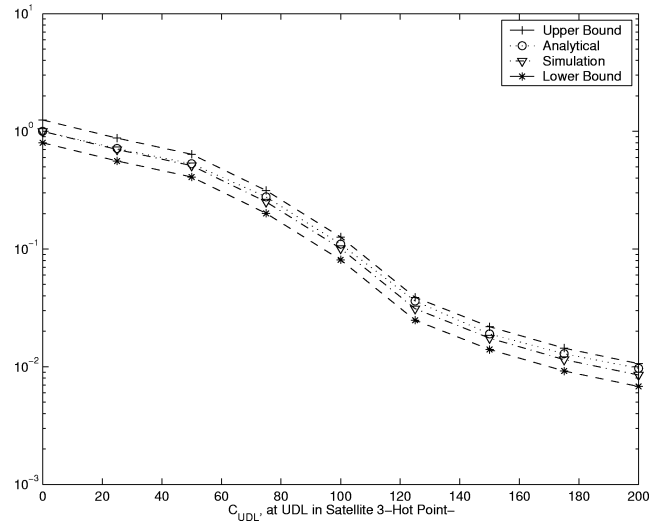

Fig. 14. Bounds, hot-spot pattern, $C_{\mathrm{ISL}} = 100, \lambda = 50, \epsilon = 0.8$ for bounds $\epsilon_{\min} = 0.85$.

algorithm for computing the link-blocking probability $P_{b,\,1}(\ell)$, as we showed in Section V. Therefore, the bounds shown in the figures are reasonably close to the "real" link-blocking probability while requiring little computational effort to obtain. As we discussed in Section V, we expect the tightness of the bounds to increase (i.e., ϵ tends to one) as the link capacity and/or the number of satellites (or satellite beams) increase. In other words, the bounds become more useful in systems in which it is computationally expensive to run the decomposition algorithm or the simulation.

VII. Concluding Remarks and Possible Extensions

We have presented an analytical model for computing call-blocking probabilities in LEO satellite networks. We have developed an algorithm for decomposing the constellation into smaller subsystems, each of which is solved in isolation using an exact method. The individual solutions are combined using an iterative scheme. We have also shown how our approach

can capture blocking due to handoffs for both satellite- and earth-fixed coverage. We have demonstrated through numerical examples that the analytical results are in good agreement with simulation. We have also derived lower and upper bounds on link-blocking probabilities that can be computed efficiently.

The analytical model we presented in this paper can be extended in several directions, some of which are the subject of current research. While in this work we have considered a fixed routing scheme, alternate routing schemes can be modeled using the techniques we developed in [13, Section IV-B]. It is also possible to improve the performance of handoff calls by reserving a set of channels on each link for the exclusive use of these calls. Channel reservation can be modeled by a modified Markov process for the single subsystem studied in Section II; we believe that a closed-form solution for the modified process can be obtained. Also, the analytical model can be extended to give priority to handoffs over new arrivals. Finally, it is possible to extend our approach to analyze the case of heterogeneous traffic (i.e., when customers are not uniformly distributed over the earth, an assumption we made in Section IV). One approach to account for different geographic arrival rates is to segment the band of earth covered by the satellites into fixed regions, each with a different arrival rate of new calls. This approach gives rise to a periodic Markov process model whose special structure can be exploited to solve it efficiently.

REFERENCES

[1] F. Dosiere, T. Zein, G. Maral, and J. P. Boutes, "A model for the handover traffic in low earth-orbiting satellite networks for personal communications," in *IEEE GLOBECOM'93*, vol. 1, Houston, TX, Nov./Dec. 1993, pp. 574–578.

[2] A. Ganz, Y. Gong, and B. Li, "Performance study of low earth orbit satellite systems," *IEEE Trans. Commun.*, vol. 42, no. 2/3/4, Feb./Mar./Apr. 1994.

[3] E. Lutz, M. Werner, and A. Jahn, *Satellite Systems for Personal and Broadband Communications*. Berlin, Germany: Springer-Verlag, 2000.

[4] V. Obradovic and S. Cigoj, "Performance evaluation of prioritized handover management for LEO mobile satellite systems with dynamic channel assignment," in *Proc. Global Telecommun. Conf.* , vol. 1a, Rio de Janeiro, Brasil, Dec. 1999, pp. 296–300.

[5] G. Pennoni and A. Ferroni, "Mobility management in LEO/ICO satellite systems: Preliminary simulation results," in *Proc. PIMRC* , vol. 4, The Hague, The Netherlands, Sept. 1994, pp. 1323–1329.

[6] E. D. Re, R. Fantacci, and G. Giambene, "Efficient dynamic channel allocation techniques with handover queueing for mobile satellite networks," *IEEE J. Select. Areas Commun.*, vol. 13, Feb. 1995.

[7] ——, "Different queueing policies for handover requests in low earth orbit mobile satellite systems," *IEEE Trans. Veh. Technol.*, vol. 48, pp. 448–458, Mar. 1999.

[8] J. Restrepo and G. Maral, "Guaranteed handover (GH) service in a nongeo constellation with 'satellite-fixed-cell' (SFC) systems," in *Proc. Int. Mobile Satellite Conf.*, Pasadena, CA, June 1997.

[9] G. Ruiz, T. L. Doumi, and J. G. Gardiner, "Teletraffic analysis and simulation of mobile satellite systems," *IEEE Trans. Veh. Technol.*, vol. 47, pp. 311–320, Feb. 1998.

[10] P. J. Wan, V. Nguyen, and H. Bai, "Advanced handovers arrangement and channel allocation in LEO satellite networks," in *Proc. Global Telecommun. Conf.*, vol. 1a, Rio de Janeiro, Brasil, Dec. 1999, pp. 286–290.

[11] A. H. Zaim, G. N. Rouskas, and H. G. Perros, "Computing call blocking probabilities in LEO satellite networks: The single orbit case," *IEEE Trans.Veh. Technol.*, vol. 51, pp. 332–347, Mar. 2002.

[12] A. Halim Zaim, "Computing call blocking probabilities in LEO satellite networks," Ph.D. dissertation, North Carolina State University, Raleigh, NC, August 2001.

[13] Y. Zhu, G. N. Rouskas, and H. G. Perros, "A path decomposition approach for computing blocking probabilities in wavelength routing networks," *IEEE/ACM Trans. Networking*, vol. 8, pp. 747–762, Dec. 2000.

Abdul Halim Zaim received the M.Sc. degree from the Computer Engineering Department, Bogazici University, Turkey, in 1996 and the Ph.D. degree from the Electrical and Computer Engineering Department, North Carolina State University, Raleigh, NC, in 2001.

As a teaching assistant, he taught several courses at Istanbul University, Istanbul, Turkey from 1993 to 1997 and from 1998 to 1999 he worked at Alcatel, Raleigh, NC. He is currently a Postdoctoral teaching associate at North Carolina State University. His research interests include computer performance evaluation, satellite and high-speed networks, and computer network design.

Harry G. Perros (M'96–SM'97) received the B.Sc. degree in mathematics in 1970 from Athens University, Athens, Greece, the M.Sc. degree in operational research with computing from Leeds University, Leeds, U.K., in 1971, and the Ph.D. degree in operations research from Trinity College, Dublin, Ireland, in 1975.

He is a Professor of computer science and Program Coordinator of the master of science degree in computer networks at North Carolina State University, Raleigh, NC. He has held visiting faculty positions at INRIA, Rocquencourt, France (1979) and University of Paris 6, Paris, France (1995–1996, 2000, and 2002). He has also spent two sabbatical terms at Nortel, Research Triangle Park, NC (1988–1989 and 1995–1996). He has published extensively in the area of performance modeling of computer and communication systems. He published a monograph entitled *Queueing Networks With Blocking: Exact and Approximate Solutions*, (Oxford, U.K.: Oxford University Press, 1994) and a textbook entitled *An Introduction to ATM Networks* (New York: Wiley, 2001). His current research interests include optical networks and satellites.

Dr. Perros has organized several national and international conferences. He is the chairman of the IFIP Working Group 6.3 on the Performance of Communication Systems and he is also a member of IFIP Working Groups 7.3 and 6.2.

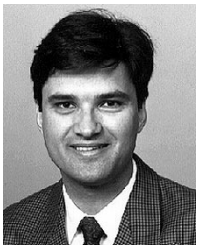

George N. Rouskas (S'92–M'95–SM'01) received the Diploma in electrical engineering from the National Technical University of Athens (NTUA), Athens, Greece, in 1989, and the M.S. and Ph.D. degrees in computer science from the College of Computing, Georgia Institute of Technology, Atlanta, GA, in 1991 and 1994, respectively.

He joined the Department of Computer Science, North Carolina State University, Raleigh, NC, in August 1994 as an Assistant Professor and he has been a Professor since July 2002. During the 2000-2001 academic year, he spent a sabbatical term at Vitesse Semiconductor, Morrisville, NC, and in May and June 2000, he was an Invited Professor at the University of Evry, Evry, France. His research interests include network architectures and protocols, optical networks, multicast communication, and performance evaluation.

Dr. Rouskas is a recipient of a 1997 NSF Faculty Early Career Development (CAREER) Award and a coauthor of a paper that received the Best Paper Award at the 1998 SPIE conference on All-Optical Networking. He also received the 1995 Outstanding New Teacher Award from the Department of Computer Science, North Carolina State University, and the 1994 Graduate Research Assistant Award from the College of Computing, Georgia Institute of Technology, Atlanta, GA. He was a coguest editor for the IEEE JOURNAL ON SELECTED AREAS IN COMMUNICATIONS Special Issue on Protocols and Architectures for Next Generation Optical WDM Networks, published in October, 2000, and is on the editorial boards of the IEEE/ACM TRANSACTIONS ON NETWORKING, *Computer Networks*, and *Optical Networks*. He is a member of the ACM and the Technical Chamber of Greece.